

Research Article

Research on Painting Image Classification Based on Transfer Learning and Feature Fusion

Qian Yong 

Dankook University, 152 Jukjeon-ro, Suji-gu, Yongin-si, Gyeonggi-do 19860, Republic of Korea

Correspondence should be addressed to Qian Yong; 2020020198@stu.cdut.edu.cn

Received 12 February 2022; Revised 21 March 2022; Accepted 24 March 2022; Published 15 June 2022

Academic Editor: Naeem Jan

Copyright © 2022 Qian Yong. This is an open access article distributed under the Creative Commons Attribution License, which permits unrestricted use, distribution, and reproduction in any medium, provided the original work is properly cited.

In order to effectively solve the problems of high error rate, long time consuming, and low accuracy of feature extraction in current painting image classification methods, a painting image classification method based on transfer learning and feature fusion was proposed. The global characteristics of the painting picture, such as color, texture, and form, are extracted. The SIFT method is used to extract the painting's local features, and the global and local characteristics are normalized and merged. The painting images are preliminarily classified using the result of feature fusion, the deterministic and non-deterministic samples are divided, and the estimated Gaussian model parameters are transferred to the target domain via a transfer learning algorithm to alter the distribution of nondeterministic samples, completing the painting image classification. Experimental results show that the proposed method has a low error rate and low feature extraction time and a high accuracy rate of painting image classification.

1. Introduction

With the continuous improvement of digital technology, more and more paintings are stored in the form of video, image, and multimedia, and anyone can use the Internet to retrieve and view paintings, which provides great convenience for people [1, 2]. The computer can properly assess the painting's distinctive characteristics, analyse, and quantify them, accurately determine its true worth and author, and even undertake an in-depth interpretation of its creative style [3]. With the fast expansion of social economics, relevant specialists and researchers have placed a greater emphasis on the categorization and identification of painting pictures in order to assess their aesthetic quality and worth, among other things. As a result, it is critical to investigate a categorization system for painting pictures [4].

For the above problems, there have been many excellent works. For example, reference [5] proposed a Chinese painting image classification method based on convolutional neural network. The design idea of this method is mainly to solve the problem that the traditional classification method has complicated feature extraction steps of painting images,

which leads to the increase in feature extraction time. Thus, the benefits of SoftSign and ReLU activation functions are combined to create a new activation function, which is then used to the convolutional neural network training process. Convolutional neural networks are used to categorise photographs of Chinese paintings. However, it is discovered that this method's classification accuracy is low in practise, and its impact is poor. Reference [6] presented a technique for classifying styles of painting based on information entropy. Using web crawler technology to collect image painting images from the database, the collected images are preprocessed to obtain higher-quality painting images, calculate the image information entropy, and classify the style of painting using a combination of the information entropy and support vector machine (SVM), but this method is too complex, and painting image feature extraction takes too long.

However, the above methods have the problems of high error rate of feature extraction, long extraction time, and low accuracy of painting image classification. Therefore, this paper proposes a new painting image classification method based on transfer learning and feature fusion.

2. Design of Painting Image Classification Method

Web crawler refers to the crawling of security rules and related data to the Web or database. Therefore, in order to improve the acquisition speed of painting images, this paper sets crawler rules and uses web crawler to capture painting images in the image database to improve the subsequent image feature extraction and classification rendering speed.

2.1. Image Feature Extraction and Fusion

2.1.1. Global Feature Extraction. Color features: HSV color space corresponds to three visual features of the human eyes, respectively. The hue range is 0–360°, which corresponds to the actual color [7, 8]. Saturation S is proportional to the degree of brightness of a color, and brightness is proportional to the ability of light. The more the energy is, the brighter the light is [9]. HSV is more closely related to human perception and experience of color than the RGB system and is thus more extensively utilised. Therefore, this paper adopts HSV color space to extract color features of painting images. This model is shown in Figure 1.

$$\begin{aligned} E_i &= \sum_{j=1}^N \frac{1}{N} p_{ij}, \\ \sigma_i &= \sqrt{\left(\frac{1}{N} \sum_{j=1}^N (p_{ij} - E_i)^2 \right)}, \\ s_i &= \sqrt[3]{\left(\frac{1}{N} \sum_{j=1}^N (p_{ij} - E_i)^3 \right)}, \end{aligned} \quad (1)$$

where i represents the total amount of color channel of the painted image, and p_{ij} represents the color value of the i -th color channel of the j -th pixel [10].

Texture features: Wavelet analysis is the most widely used method in extracting image texture features [11]. This method is very stable in signal processing and has shown good results in many research fields, with broad application prospects. The principle of texture feature extraction using wavelet transform is shown in Figure 2.

The classical wavelet functions include Haar, Morlet, dbn, and sym N. The following is a brief introduction to Haar wavelet functions. The definition is shown in the following formula:

$$\psi(t) = \begin{cases} 1, & 0 \leq t \leq \frac{1}{2}, \\ -1, & \frac{1}{2} \leq t \leq 1, \\ 0, & \text{otherwise.} \end{cases} \quad (2)$$

Let kernel function $\psi(x)$ be the female wavelet, and a cluster of orthogonal basis can be obtained through translation and scaling [12].

$$\psi_{m,n}(x) = 2^{-m/2} \psi(2^{-m}x - n). \quad (3)$$

Then, the wavelet coefficients of the signal $f(x)$ can be expressed by the following formula:

$$c_{m,n} = \int_{-\infty}^{\infty} f(x) \psi_{m,n}(s) dx. \quad (4)$$

If the scale function $\phi(x)$ satisfies the two-scale difference equation [13], it can be expressed as follows:

$$\phi(x) = \sqrt{2} \sum_k h(k) \phi(2x - k). \quad (5)$$

Then, the relation between the wavelet kernel function $\psi(x)$ and the scale function is

$$\psi(x) = \sqrt{2} \sum_k g(k) \phi(2x - k), \quad g(k) = (-1)^k h(1 - k). \quad (6)$$

Explicit $\phi(x)$, $\psi(x)$ are not required for wavelet transformation but depend on $h(k)$, $g(k)$. A J -order wavelet decomposition can be written as follows:

$$f_0(x) = \sum_k c_{0,k}(x) = \sum_k \left(c_{j+1,k} \phi_{j+1,k}(x) + \sum_{j=0}^j d_{n+1,k} \phi_{n+1,k}(x) \right). \quad (7)$$

If the coefficient $c_{0,k}$ is known, the relationship between the coefficient of grade $j+1$ and that of grade j is [14]

$$\begin{aligned} c_{j+1,n} &= \sum_k c_{j,k} h(k - 2n), \\ d_{j+1,n} &= \sum_k c_{j,k} g(k - 2n). \end{aligned} \quad (8)$$

Combined with the above analysis, the wavelet coefficient $d_{j,n}$ is used to construct the recursive algorithm, which is described as follows:

$$c_{j,k} = \sum_n c_{j+1,n} h(k - 2n) + \sum_n d_{j+1,n} g(k - 2n). \quad (9)$$

Let $\bar{h}(n)$ and $\bar{g}(n)$ be signals with impulse response and use their high and low filters to sample filter signals and combine them to achieve wavelet transform [15]. $\bar{h}(n)$ and $\bar{g}(n)$ are defined as follows:

$$\bar{h}(n) = h(-n), \quad \bar{g}(n) = g(-n). \quad (10)$$

In two-dimensional signal, the small and medium wave function can be expressed as

$$\begin{cases} \phi(x, y) = \phi(x)\phi(y), \\ \psi^1(x, y) = \phi(x)\psi(y), \\ \psi^2(x, y) = \psi(x)\phi(y), \\ \psi^3(x, y) = \psi(x)\psi(y). \end{cases} \quad (11)$$

The corresponding two-dimensional filtering function is

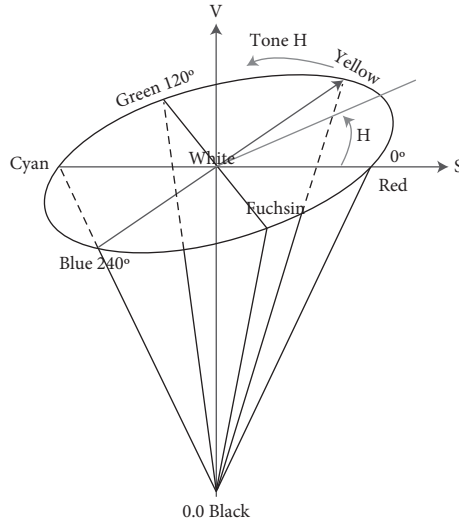


FIGURE 1: HSV color space model.

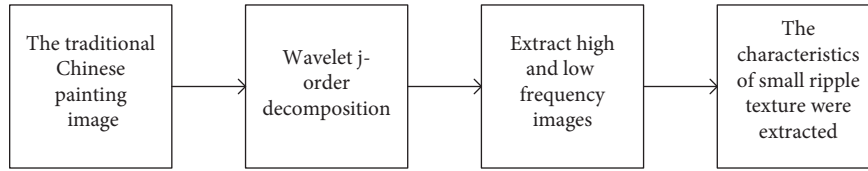


FIGURE 2: Flow chart of wavelet transform.

$$\begin{cases} h_{LL}(k, l) = h(k)h(l), \\ h_{LH}(k, l) = h(k)g(l), \\ h_{HL}(k, l) = g(k)h(l), \\ h_{HH}(k, l) = g(k)g(l). \end{cases} \quad (12)$$

The image is set as $f(x, y)$, and the wavelet decomposition process of the image is shown in Figure 3 [16, 17].

Texture features are the result of frequency variations in all directions. Firstly, the traditional Chinese painting is decomposed into four components: LL, LH, HL, and HH. LL1 was decomposed and sampled to obtain second-order wavelet decomposition, as shown in Figure 4 [18]. And, if further decomposition is required to obtain more vector information, the same operation is continued for LL2.

Shape features: Compared with color and texture features, shape features belong to deeper image features. Therefore, in order to improve the extraction accuracy of painting image shape features, this paper uses Fourier shape descriptors [19, 20] to achieve this important goal.

Suppose in XY there is a boundary in the plane, the boundary mainly consists of N coordinates for (x_n, y_n) points, the starting point at this point, moving counter-clockwise along the border, will form the multiple trajectories, mainly expressed in $(x_0, y_0), (x_1, y_1), \dots, (x_{n-1}, y_{n-1})$, at this time will be XY plane and complex plane UV overlap, and redefine the boundary points, as shown in Figure 5.

$$s(n) = x(n) + jy(n), n = 1, 2, \dots, N - 1. \quad (13)$$

The discrete Fourier transform of $s(n)$ [21, 22] is

$$S(w) = \frac{1}{N} \sum_{n=0}^{N-1} s(n) \exp\left(-j \frac{2\pi wn}{N}\right), \quad w = 0, 1, \dots, N - 1. \quad (14)$$

The inverse Fourier transform of $S(w)$ is

$$S(k) = \sum_{w=0}^{N-1} S(w) \exp\left(-j \frac{2\pi wk}{N}\right), \quad k = 0, 1, \dots, N - 1. \quad (15)$$

If only the first P coefficients of $S(w)$ are selected here, namely $P \leq N - 1$, another similar expression of $S(k)$ can be derived, namely the Fourier shape descriptor.

$$\hat{S}(k) = \sum_{w=0}^{P-1} S(w) \exp\left(-j \frac{2\pi wk}{N}\right), \quad k = 0, 1, \dots, N - 1. \quad (16)$$

The shape features vector of the painting image is described by the Fourier shape descriptor, and the shape feature of the painting image is extracted.

2.1.2. Local Feature Extraction Based on SIFT Algorithm. Scale-invariant feature transform (SIFT) is a classical shape feature and belongs to a local feature algorithm. Local features extracted have invariance and stability [23]. The specific process is as follows.

Extreme value detection of scale space: The scale-space kernel is defined as follows:

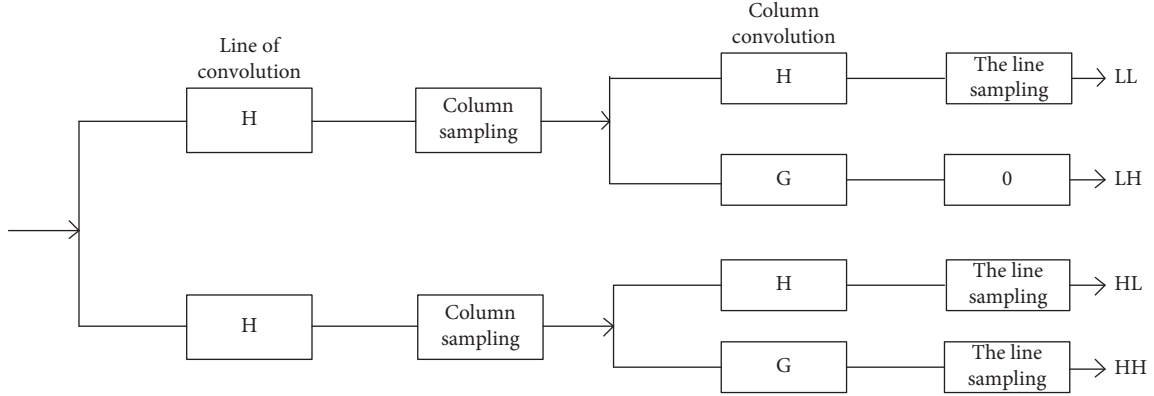


FIGURE 3: Schematic diagram of wavelet decomposition.

The approximate weight LL1	Vertical component HL1	LL2	HL2	HL1
		LH2	HH2	
Horizontal component LH1	The diagonal components HH1	LH1		HH1

FIGURE 4: First-order and second-order decomposition coefficients.

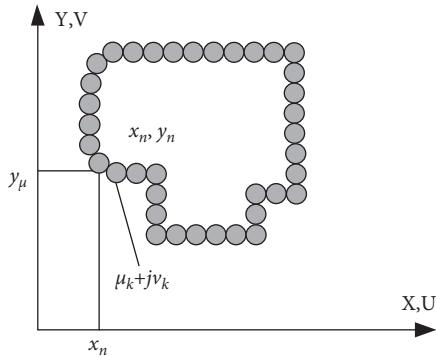


FIGURE 5: Two representations of boundary points.

$$f_{\text{out}} = K * f_{\text{in}}, \quad (17)$$

where $*$ represents convolution operation, and K represents scale-space kernel. Gaussian difference scale space can be obtained by using this parameter, as follows:

$$\begin{aligned} D(x, y, \sigma) &= (G(x, y, k\sigma) - G(x, y, \sigma)) * I(x, y), \\ &= L(x, y, k\sigma) - L(x, y, \sigma). \end{aligned} \quad (18)$$

Among them,

$$G(x, y, \sigma) = \frac{1}{2\pi\sigma^2} e^{-((x^2+y^2))/2\sigma^2}, \quad (19)$$

where σ is the standard deviation of the Gaussian kernel, and (x, y) is the spatial coordinate point of an image $I(x, y)$.

Positioning of key points: Key points are selected according to the scale and stability of candidate points. If the value of operation comparison is greater than or less than all

adjacent points, the candidate point is identified as the key point [24]

Key point direction assignment: After the key point is found, one or more directions are assigned to its local image gradient. Taylor's expansion (fitting function) corresponding to the Gaussian function is

$$D(x) = D + \frac{\partial D^T}{\partial x} x + \frac{1}{2} x^T \frac{\partial^2 D}{\partial x^2} x. \quad (20)$$

For alternative points D and D' , $D' = 0$, x , and the corresponding $D(x)$ are calculated, and the threshold is set as follows:

$$x = - \left[\frac{\partial^2 D}{\partial x^2} \right]^{-1} \frac{\partial D}{\partial x}, \quad (21)$$

$$D(x) = D + \infty \frac{1}{2} \frac{\partial D^T}{\partial x} x.$$

The Hessian matrix 2×2 at the "feature point" with constant scale [25] is obtained, and the trace and determinant of the 2×2 -dimensional Hessian matrix $\begin{bmatrix} D_{xx} & D_{xy} \\ D_{xy} & D_{yy} \end{bmatrix}$ are solved.

$$\begin{aligned} \text{Tr}(H) &= D_{xx} + D_{yy} = \alpha + \beta, \\ \text{Det}(H) &= D_{xx} + D_{yy} - (D_{xy})^2 = \alpha\beta. \end{aligned} \quad (22)$$

Discard the edge response point, set γ as the ratio of two characteristic values, have $\alpha = \gamma\beta$, then the following relationship exists:

$$\frac{\text{Tr}(H)^2}{\text{Det}(H)} = \frac{(\alpha + \beta)^2}{\alpha\beta} = \frac{(r\alpha + \beta)^2}{r\beta^2} = \frac{(R + 1)^2}{R}. \quad (23)$$

Feature points are judged by the threshold, more representative feature points are selected, and unstable key points are screened.

$$\frac{\text{Tr}(H)^2}{\text{Det}(H)} < \frac{(R + 1)^2}{R}. \quad (24)$$

Generate descriptors: From the local picture gradient information, a descriptor is constructed for each key point, and its scale is determined in the second step. The critical element is that the algorithm creates a huge number of

highly distinctive characteristics in a variety of sizes and places [26]. The gradient's modulus and direction are as follows:

$$m(x, y) = \sqrt{(L((x+1), y) - L((x-1), y))^2 + (L(x, (y+1)) - L(x, (y-1)))^2},$$

$$\theta(x, y) = \arctan \left[\frac{L(x, (y+1)) - L(x, (y-1))}{L((x+1), y) - L((x-1), y)} \right]. \quad (25)$$

The local feature extraction of the painting image is realized by generating descriptors to describe the local feature of the painting image.

2.1.3. Feature Fusion. In the process of painting image classification, not all feature descriptors have the same classification and discrimination ability for each category. For example, texture features can be used to classify different leaves well, but color features cannot achieve the same effect. Considering that texture features and shape features have different contributions to the classification of debris in different parts, multifeature fusion is needed to highlight the influence of different image features in different parts.

Given a target image, its global feature vector $C_q = [C_q(1), C_q(2), \dots, C_q(m)]$ and local feature vector $M_q = [M_q(1), M_q(2), \dots, M_q(m)]$ are extracted where m and n represent the dimensions of the two feature vectors, respectively.

Due to the different dimensions of global feature and local feature algorithms, there will be differences when using similarity measurement algorithms. In order to avoid this trouble, C_q and M_q need to be normalized, and the formula is as follows:

$$D'_C(i) = \frac{D_C(i)}{\max(D_C(i)) - \min(D_C(i))}, \quad i = 1, 2, \dots, N,$$

$$D'_M(i) = \frac{D_M(i)}{\max(D_M(i)) - \min(D_M(i))}, \quad i = 1, 2, \dots, M, \quad (26)$$

where $D_C(i)$ and $D_M(i)$ represent the distance between the original global feature and local feature and the corresponding feature of the sample image. $D'_C(i)$ and $D'_M(i)$ represent the normalized results of $D_C(i)$ and $D_M(i)$, and N represents the number of images stored in the image database.

Let Q_q represents the features after fusion of the two features, w_1 is the weight of global features, and w_2 is the weight of local features, and then, the features after fusion can be expressed by the following formula:

$$Q_q = w_1 D'_C(i) + w_2 D'_M(i). \quad (27)$$

2.2. Painting Image Classification Based on Transfer Learning. Transfer learning is a kind of machine learning algorithm whose primary objective is to derive new domain knowledge

from previously acquired domain information. By using current information in the source domain to acquire unknown knowledge in the target domain, the acquisition of target domain knowledge is no longer a zero-sum game and may significantly boost the target domain's learning impact. The transfer learning algorithm's fundamental flow chart is shown in Figure 6

Based on the result of feature fusion, the painting images are preliminarily classified, the deterministic samples and the nondeterministic samples are divided, and the parameters of the Gaussian model estimated are transferred to the target domain by the transfer learning algorithm to change the distribution of nondeterministic samples, so as to obtain accurate painting image classification results.

Assuming that the painting image sample to be classified is called the target domain D_T , the specific process of dividing D_T is as follows:

Step 1K-means clustering algorithm is used to cluster sample D_T in the target domain to obtain different painting image sample category labels;

Step 2Assume that the purpose of painting image classification is to divide painting images into k categories, the label vectors of two different classification results are λ_a and λ_b , and the results of painting image classification are $\{C_{a1}, C_{a2}, \dots, C_{ak}\}$ and $\{C_{b1}, C_{b2}, \dots, C_{bk}\}$. Then, a symmetric matrix S with a size of $k \times k$ can be obtained, and the value in it represents the number of overlaps between classes. When the value is the largest, the category labels of the two classes are the same, and the matching results of all classes can be obtained after repeated for many times.

Step 3After the successful matching of category labels, the clustering consistency value CI is introduced for the effective discriminative sample D_A and nondeterministic sample D_B , which is mainly calculated by the following formula:

$$CI(x) = \frac{1}{H} \max \left\{ \sum_{t=1}^H \delta(\pi_t(x), L) \right\}, \quad (28)$$

where H represents the number of clustering, $\pi_t(x)$ represents the classification result of painting image sample x in the t -th classification, and L represents each category identification.

Step 4Set a threshold value of Q , and take samples of $CI \geq Q$ as deterministic samples D_A , and samples of $CI < Q$ as nondeterministic samples D_B ;

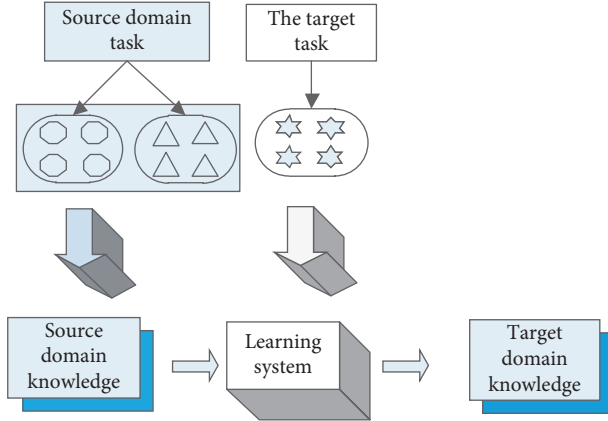


FIGURE 6: Basic flow chart of migration algorithm.

Step 5 According to the obtained clustering results, record the categorical label of the deterministic sample, which is recorded as l_a .

After the division of the above steps, we have obtained the deterministic sample D_A , the nondeterministic sample D_B , and the label l_a of the deterministic sample. What we need to do now is to change the painting image classification results of the nondeterministic sample D_B by migrating the sample distribution of the source domain D_s . The following is how to transfer the parameters of the mixed Gaussian model (GMM) of the source domain to the target domain using the transfer learning algorithm:

- (i) Step 1: the parameters of the mixed Gaussian model are estimated, and the quasimixing parameters, mean value, and covariance of the mixed Gaussian model in the source domain are α_j , μ_j , and σ_j

Step 2: according to the numbers α_j , μ_j , and σ_j , calculate the membership function Z in the source domain, and the calculation formula of membership Z is as follows:

$$Z_{i,j} = \frac{\alpha_j G(X_i; \mu_j, \sigma_j)}{\sum_{j=1}^k \alpha_j G(X_i; \mu_j, \sigma_j)}, \quad (29)$$

where $i = m \times n$ is the number of samples, and $j = 1, 2, \dots, k$, k are the number of categories

Step 3: use the membership degree $Z_{i,j}$ calculated above to calculate the mixed Gaussian parameter $\alpha_{j_{new}}$, mean $\mu_{j_{new}}$, and covariance $\sigma_{j_{new}}$ of the sample under this membership degree in the target domain sample D_T , and the calculation formulas are as follows:

$$\begin{aligned} \alpha_{j_{new}} &= \frac{1}{n} \sum_{i=1}^n Z_{i,j}, \\ \mu_{j_{new}} &= \frac{\sum_{i=1}^n Z_{i,j} X_i}{\sum_{i=1}^n Z_{i,j}}, \\ \sigma_{j_{new}} &= \frac{\sum_{i=1}^n Z_{i,j} (X_i - \mu_j)(X_i - \mu_j)^T}{\sum_{i=1}^n Z_{i,j}}. \end{aligned} \quad (30)$$

The new Gaussian mixture model parameters $\alpha_{j_{new}}$, $\mu_{j_{new}}$, and $\sigma_{j_{new}}$ were used to calculate the membership function $Z'_{i,j}$ of the target domain D_T , thus completing the task of migrating the parameters of sample points in the source domain to the target domain.

Step 4: substitute the new parameter into the Gaussian distribution formula to obtain the probability value of each sample in D_B , so as to obtain the classification result of D_B images 88, namely the classification result of painting images.

The specific implementation steps of painting image classification are shown in Figure 7.

- (1) Determine the number of deterministic and non-deterministic samples based on feature fusion results and cluster consistency values
- (2) Determine the number of deterministic and non-deterministic samples based on feature fusion results and cluster consistency values
- (3) Determine the number of deterministic and non-deterministic samples based on feature fusion results and cluster consistency values
- (4) The source domain is picked at random from the remaining bands of the data, and the GMM parameters in the source domain are estimated
- (5) The calculated parameters are transferred to the target domain to modify the distribution of the nondeterministic sample
- (6) After calculating the final clustering result, Dunn's index was used to generate the clustering validity value, which was then compared to the initial clustering validity value
- (7) If the clustering effectiveness decreases, repeat the above three steps and then reselect the source region for migration until a good painting image classification effect is achieved.

3. Experimental Design

In order to verify the validity of the painting image classification method based on transfer learning and feature fusion designed in this paper, relevant experimental tests are carried out, and the experimental environmental parameters are shown in Table 1.

In the network, crawler technology is used to crawl 10000 painting images, and all data are denoised. The sample images after denoising are taken as experimental sample images, part of which are shown in Figure 8.

Reference [5] proposed a painting image classification method based on convolution neural networks, reference [6] proposed a painting image classification method based on information entropy, and this paper proposed a painting image classification method based on transfer learning and feature fusion as an experiment contrast method, by comparing different experimental indexes to verify the application effect of different methods.

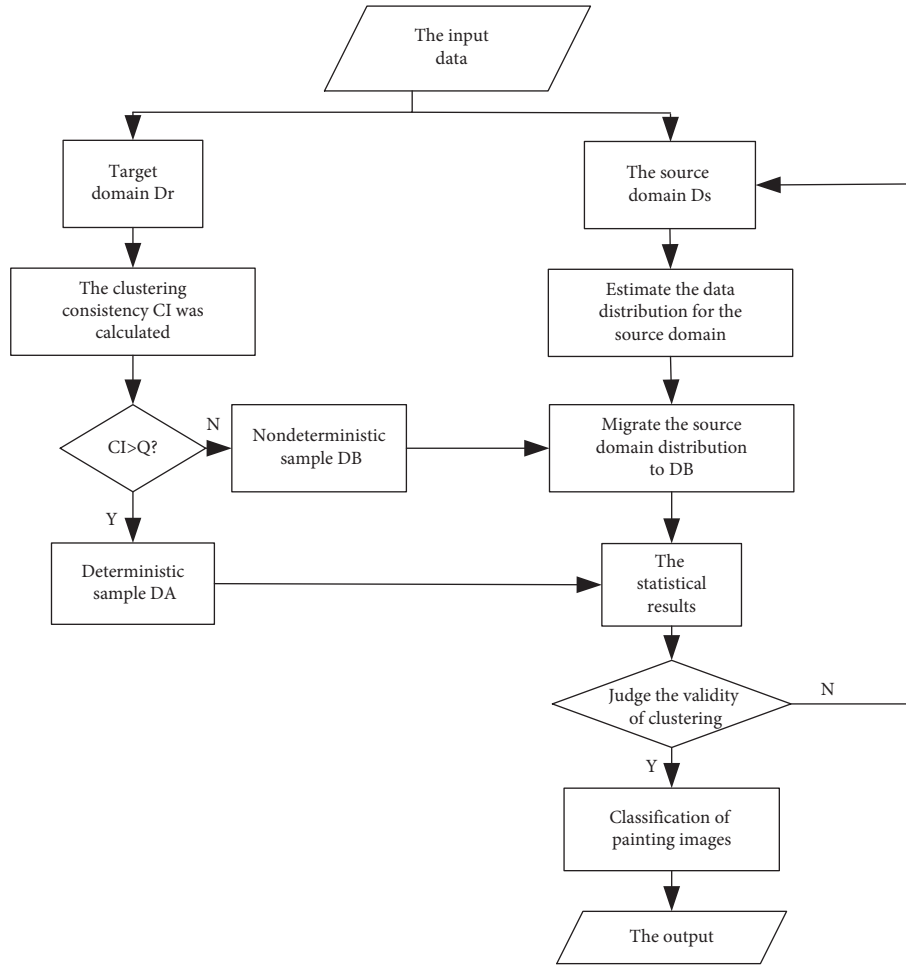


FIGURE 7: Specific implementation steps of painting image classification.

TABLE 1: Experimental environmental parameters.

The name of the	Parameter
Operating system	Windows 10
CPU	Intel core i5-7300HQ
Memory	32G
Hard disk	500 GB
Run a memory	8G
Frequency	2.1 GHz
Simulation software	Matlab R2014a

3.1. *A Comparison of Feature Extraction Error Rates.* Figure 9 compares the feature extraction error rate of painting pictures using the convolutional neural network classification technique, the information entropy-based classification approach, and the classification method based on transfer learning and feature fusion.

Analysis of the data in Figure 9 shows that the error rate of feature extraction of painting image based on convolutional neural network is between 13% and 20%, that of feature extraction of painting image based on information entropy is between -17% and 2%, and that of feature extraction of painting image based on transfer learning and feature fusion is between 2% and 4%. It shows that the

feature extraction accuracy of the proposed method is higher, which can lay a foundation for the subsequent feature classification of painting images.

3.2. *Feature Extraction Time Comparison.* The feature extraction time of painting images based on convolutional neural network classification method, information entropy-based classification method, and classification method based on transfer learning and feature fusion is compared, and the results are shown in Figure 10.

As shown in Figure 10, as the number of tests increases, the time it takes to extract painting attributes from various approaches varies. The classification approach based on convolutional neural networks has a maximum and lowest time of feature extraction of 4.0s and 2.0s, respectively. The greatest and lowest times for feature extraction based on information entropy are, respectively, 3.9s and 1.7s. The maximum time and minimum time of feature extraction of painting image based on the classification method of transfer learning and feature fusion are 0.7s and 0.5s, respectively. Compared with the experimental comparison method, feature extraction of painting image in this paper is shorter and more efficient.



FIGURE 8: Images of some experimental samples.

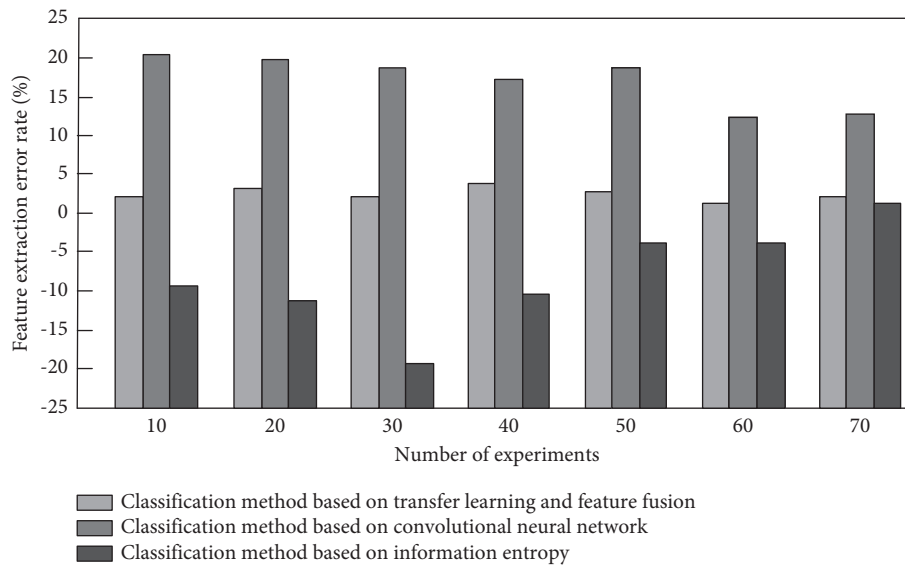


FIGURE 9: Comparison of error rates of feature extraction.

3.3. *Classification and Comparison of Painting Images.* The accuracy of painting image classification based on convolutional neural network, information entropy, and transfer learning and feature fusion is compared, and the comparison results are shown in Table 2.

By analyzing the comparison results of the accuracy of painting image classification in Table 2, it can be seen that

the average accuracy of painting image classification based on convolutional neural network is 84.35%, and that of painting image classification based on information entropy is 77.76%. The average accuracy rate of painting image classification based on transfer learning and feature fusion is 96.72%, indicating that the classification result of this method is more accurate.

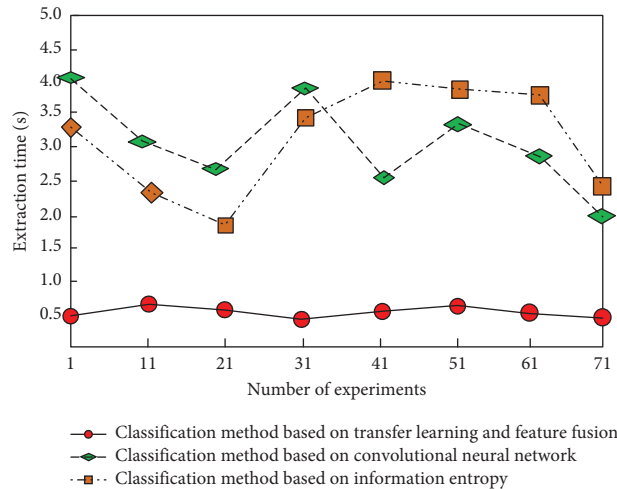


FIGURE 10: Comparison of painting feature extraction time.

TABLE 2: Comparison of classification accuracy of painting images (unit:%).

Number of experiment	Classification method based on convolutional neural network	Classification method based on information entropy	Classification method based on transfer learning and feature fusion
10	85.63	79.56	98.75
20	84.75	78.81	96.31
30	81.55	75.66	97.48
40	83.24	74.12	95.37
50	84.75	85.32	95.44
60	86.33	74.33	97.14
70	84.17	76.55	96.52
Average	84.35	77.76	96.72

4. Conclusion

In the development of human civilization, the painting is the precious spiritual wealth. Through exquisite painting, it can fully display the rich spirit of the era. The present stage of painting gradually moves towards the direction of the digital and intelligent, so a lot of drawing is carried out in the network. The classification of the painting according to the content of the painting style is particularly important. Therefore, this paper introduces transfer learning and feature fusion methods to design a new painting image classification method. Experimental results show that the error rate of feature extraction of painting images in this method ranges from 2% to 4%, the maximum time of feature extraction is 0.7s, the minimum is 0.5s, and the average accuracy rate of painting image classification is 96.72%, indicating that this method can not only achieve accurate and rapid feature extraction of painting images but also achieve the correct classification of painting images. It can lay a solid foundation for the development of painting image classification.

Data Availability

The data used to support the findings of this study are included within the article.

Conflicts of Interest

The authors declare that they have no conflicts of interest.

References

- [1] N. Wei, "Research on the algorithm of painting image style feature extraction based on intelligent vision," *Future Generation Computer Systems*, vol. 123, no. 24, pp. 196–200, 2021.
- [2] Y. Zhang, "Research on digital image technology in oil painting image processing," *IOP Conference Series: Materials Science and Engineering*, vol. 750, no. 1, pp. 012096–012112, 2020.
- [3] D. Li and Y. Zhang, "Multi-instance learning algorithm based on LSTM for Chinese painting image classification," *IEEE Access*, vol. 8, no. 1, pp. 179336–179345, 2020.
- [4] T. Lee, D. K. Kang, K. Yoon, and S. Seo, "Emotion-based painting image display system," *Intelligent Automation and Soft Computing*, vol. 15, no. 1, pp. 181–192, 2019.
- [5] B. Yang, H. Y. Chen, X. H. Wang, and J. L. Yao, "Chinese painting image classification based on convolutional neural network," *Software Guide*, vol. 18, no. 1, pp. 5–8, 2019.
- [6] W. H. Qian, D. Xu, J. Xu, L. He, and Z. Y. Han, "Research on classification of Style painting based on information entropy," *Journal of Graphics*, vol. 40, no. 6, pp. 991–999, 2019.
- [7] Y. T. Zhou, "Chinese painting image classification method based on improved convolutional neural network model," *Journal of Jiamusi University (Natural Science Edition)*, vol. 39, no. 1, pp. 112–115, 2019.

- [8] K. Shirai, Y. Ito, H. Miyao, and M. Maruyama, "Efficient pixel-wise SVD required for image processing using the color line feature," *IEEE Access*, vol. 2021, no. 99, pp. 1–10, 2021.
- [9] J. Chaki and N. Dey, "Introduction to image color feature," *Image Color Feature Extraction Techniques*, vol. 78, no. 1, pp. 1–28, 2020.
- [10] Y. Li, C. Ma, and T. Zhang, "Underwater image high definition display using the multilayer perceptron and color feature-based SRCNN," *IEEE Access*, vol. 7, no. 1, pp. 83721–83728, 2019.
- [11] Z. Zhao, T. Liu, and X. Zhao, "Variable selection from image texture feature for automatic classification of concrete surface voids," *Computational Intelligence and Neuroscience*, vol. 2021, no. 1, pp. 1–10, 2021.
- [12] A. M. Shamaileh, T. H. Rassem, L. S. Chuin, and O. N. Al Sayaydeh, "A new feature-based wavelet completed local ternary pattern (Feat-WCLTP) for texture image classification," *IEEE Access*, vol. 8, no. 1, pp. 1–12, 2020.
- [13] Q. Zhang and Y. Li, "Medical image segmentation algorithm based on multi-scale color wavelet texture," *International Journal of Circuits, Systems and Signal Processing*, vol. 15, no. 2, pp. 928–935, 2021.
- [14] Y. Liu, B. Zhou, and X. Yang, "Wavelet analysis-based texture analysis of ceramic surface images," *Advances in Mathematical Physics*, vol. 2021, no. 10, pp. 1–11, 2021.
- [15] Y. Benlcouiri, M. C. Ismaili, and A. Azizi, "Crypto-watermarking of images based on the permutation on Z/pZ and the wavelet decompositions of legall 5/3," *Journal of Computer Science*, vol. 15, no. 6, pp. 855–860, 2019.
- [16] U. A. Nnolim, "Single image de-hazing via multiscale wavelet decomposition and estimation with fractional gradient-anisotropic diffusion fusion," *International Journal of Image and Graphics*, vol. 21, no. 3, pp. 127–136, 2021.
- [17] L. Chen, J. Li, Y. Zeng, Y. Chen, and W. Liang, "Magnetic flux leakage image enhancement using bidimensional empirical mode decomposition with wavelet transform method in oil pipeline nondestructive evaluation," *Journal of Magnetism*, vol. 24, no. 3, pp. 423–428, 2019.
- [18] A. Muthukrishnan, J. Kumar, D. V. Kumar, and M. Kanagaraj, "Internet of image things-discrete wavelet transform and Gabor wavelet transform based image enhancement resolution technique for IoT satellite applications," *Cognitive Systems Research*, vol. 57, no. 1, pp. 46–53, 2019.
- [19] G. Sun and X. U. Liang, "Clothing style recognition approach based on the accurate Fourier height functions shape descriptor," *China Measurement & Test*, vol. 45, no. 8, pp. 130–134, 2019.
- [20] R. P. Gentallan, N. C. Altoveros, T. H. Borromeo et al., "An objective method of shape descriptor state establishment using elliptic Fourier analysis (EFA)," *Plant Genetic Resources*, vol. 17, no. 6, pp. 1–10, 2019.
- [21] N. A. Harthi, Z. Zhang, D. Kim, and S. Choi, "Peak-to-Average power ratio reduction method based on partial transmit sequence and discrete fourier transform spreading," *Electronics*, vol. 10, no. 6, pp. 642–653, 2021.
- [22] H. Konno, A. Dobroui, S. Suzuki, M. Asada, and H. Ito, "Discrete fourier transform radar in the terahertz-wave range based on a resonant-tunneling-diode oscillator," *Sensors*, vol. 21, no. 13, pp. 4367–4379, 2021.
- [23] T. Liu, "Building recognition system based on improved SIFT algorithm and positioning information," *Journal of Image and Signal Processing*, vol. 10, no. 3, pp. 106–112, 2021.
- [24] Y. J. Yu, G. F. Wang, and J. Zhao, "FI-SIFT algorithm for exposing image copy-move forgery with reflection attacks," *International Journal on Network Security*, vol. 22, no. 2, pp. 183–190, 2020.
- [25] X. F. Liao, X. C. Zhuang, W. Gong, and J. Chen, "SIFT feature extraction and matching algorithm based on sequence minimum optimization," *Computer Simulation*, vol. 36, no. 2, pp. 219–223, 2019.
- [26] S. Paul and U. C. Pati, "SAR image registration using an improved SAR-SIFT algorithm and delaunay-triangulation-based local matching," *IEEE Journal of selected topics in applied earth observations and remote sensing*, vol. 12, no. 8, pp. 2958–2966, 2019.